

# Rheology and Viscosity Prediction of Bituminous Coal Slag in Reducing Atmosphere

Feng Zhao, Jie Xu, Wei Huo, Fuchen Wang and Guangsuo Yu\*

Key Laboratory of Coal Gasification, Ministry of Education, Shanghai Engineering Research Center of Coal Gasification, East China University of Science and Technology, Shanghai, PR China

## Abstract

The high-temperature rheology of bituminous coal slag in the reducing atmosphere was investigated in this study. The characteristics of slag sample were analyzed by multi-techniques. The rheological measurement of the slag was carried out by a high-temperature rheometer at temperatures of 1360-1460°C. The effects of the shear rate and temperature on the rheological property of the slag were studied. The volume fractions of crystallize particles and mineral matters variation were predicted by thermodynamic software FactSage. The results show that the viscosity and shear stress of the slag increase with decreasing temperature at the constant shear rate. When the volume fraction of the crystallize particles is less than 10%, the slag behaves as a Newtonian fluid. When the volume fraction of the crystallize particles is more than 15%, the slag viscosity decreases with increasing shear rate. The non-Newtonian fluid behavior of slag is illustrated by shear thinning behavior and thixotropic behavior. With decreasing temperature, the shear thinning behavior becomes increasingly significant. In addition, the viscosity prediction model basing on S2 model and Einstein-Roscoe model was established.

**Keywords:** Rheology of slag; Viscosity; Reducing atmosphere; FactSage; Gasification

## Introduction

Coal gasification is an important coal conversion technology which has been commercially used to produce fuels and chemicals [1]. Among various types of gasifiers, the developments of entrained-flow gasification for employing slagging technology to produce the syngas have been driven by a demand for higher efficiency and lower greenhouse gas emissions [2,3]. In the entrained-flow gasifier, pulverized coal is gasified and its mineral matters are converted into ash. Then the ash melts and forms a slag layer which flows to the bottom along the inner wall because of gravity and then out of the gasifier [4-7]. In general, the accepted viscosity for successful slagging of the gasifier is typically less than 25 Pa·s [8]. In order to successful slagging, the operation temperature must be higher than the temperature when the viscosity is 25 Pa·s. In addition, the suitable operation temperature can reduce oxygen and feedstock consumptions, extend refractory life and reduce costs, which is beneficial to yield product efficiently [9]. However, determination of the operational condition is not only closely related to the slagging viscosity but also to the rheology of slag, because the characters of rheology can be used to predict the change of viscosity. Therefore, a good understanding of the slag rheology is essential to determine the operation temperature and thus enable stable long-term operation of entrained-flow gasifier. At high temperature, the slag contains large amounts of molten phases and it can be regarded as Newtonian fluid. With decreasing of the temperature, the slag is cooled and the crystallized particles form. Thus, the fluid is comprised of a mix of solid phase and liquid phase and behaves non-Newtonian characteristics [10].

Numerous studies on the slag viscosity have been reported [11-14]. Wall et al. [15] used a thermomechanical analysis apparatus to measure slag viscosity at high temperatures. Nowok et al. [16,17] investigated the effects of atmosphere and local structure of a lignitic coal slag on viscosity. Schobert et al. [18,19] reported the fluidity of slag under different atmospheres and flow properties of laboratory ash in a reducing atmosphere. However, little work has been investigated on the rheology of slag, except the studies reported by Tomukayakul et al.

[20] and Song et al. [21]. Tomukayakul et al. [20] discussed the effect of shear rate on the shear stress and apparent viscosity of laboratory ashes at different temperatures. Song et al. [21] investigated the rheological properties of Texaco gasifier slag in oxidizing atmosphere. But the reducing atmosphere which fills in the actual operation of the entrained-flow gasifier has not been studied. Due to the complex procedure and more time consumption of the viscosity test, models on viscosity estimation have been set up and widely used, such as the S<sup>2</sup>, Watt-Fereday, Shaw, Urbain, modified Urbain, Riboud, Streeter, Kalmanovitch-Frank and Nicholls-Reid models [10]. Hence, it is necessary to study the rheology and viscosity prediction of slag in reducing atmosphere.

In this study, the rheology of slag prepared in laboratory was measured under reducing atmosphere with 60% volume CO and 40% volume CO<sub>2</sub> to simulate the industrial environment in the gasifier. The chemical composition, mineral analysis, and microstructure of slag were carried out by X-ray fluorescence (XRF), X-ray diffraction (XRD) and scanning electron microscopy (SEM). The rheological behavior and thixotropic behavior of slag at different temperatures were investigated by high-temperature rheometer. The thermodynamic software FactSage was used to calculate the volume fraction of crystalline particles in the slag and the mineral matters content variation with the change of temperature. Moreover, the fluid models at different temperatures were established and the viscosity of slag was predicted.

**\*Corresponding author:** Guangsuo Yu, Key Laboratory of Coal Gasification, Ministry of Education, Shanghai Engineering Research Center of Coal Gasification, East China University of Science and Technology, Shanghai 200237, PR China, Tel: 862164252974; E-mail: [gsyu@ecust.edu.cn](mailto:gsyu@ecust.edu.cn)

**Received** September 02, 2015; **Accepted** September 16, 2015; **Published** September 23, 2015

**Citation:** Zhao F, Xu J, Huo W, Wang F, Yu G (2015) Rheology and Viscosity Prediction of Bituminous Coal Slag in Reducing Atmosphere. J Chem Eng Process Technol 6: 243. doi:10.4172/2157-7048.1000243

**Copyright:** © 2015 Zhao F, et al. This is an open-access article distributed under the terms of the Creative Commons Attribution License, which permits unrestricted use, distribution, and reproduction in any medium, provided the original author and source are credited.

## Experimental

### Slag preparation

In this work, the representative Chinese bituminous coal, Yulin coal, was chosen. Yulin coal is widely used in the coal gasification. Yulin coal was processed in a muffle furnace at 815°C for 1 hour according to the Chinese standard GB/T212-2008. Then the coal ash was fused in high temperature furnace to get the slag sample. The slag was milled to a particle size about 50  $\mu\text{m}$  for XRF and XRD analysis.

### The characterization of slag

The composition of slag was measured by X-ray fluorescence spectrometer. The mineral constituent of slag was analyzed by X-ray diffractometer. The microstructure of slag was determined by scanning electron microscope.

### Measurement of rheology and viscosity

**Experimental apparatus:** The high-temperature rotational viscometer was employed for rheology and viscosity measurement in this study. The schematic diagram of high-temperature rotational viscometer is shown schematically in Figure 1. The rotating concentric cylinder principle was used in the measuring system. The rotating bob rheometer was a Brookfield programmable rheometer with a measuring head. The spindle immersed in the molten sample was driven by a spring in the rheometer. Then the viscosity of sample against spindle was measured by spring distortion. The spring distortion was converted into an electrical signal by a rotary transducer. The sample in a vertical furnace was heated to the required temperature. The furnace temperature was controlled by programmable software and the experimental data were recorded by a computer. To simulate the actual conditions in the gasifier, the mixture of  $\text{CO}_2$  and  $\text{CO}$  with volume ratio 4/6 was injected into the system.

The bob was calibrated by Brookfield standard oil at room temperature in the range of actual rotation rates and at high-temperature with a standard borosilicate glass which was used as reference material for high-temperature viscosity measurements. The mean measured deviation of the viscosity determined in experiment was no more than 4%.

**Viscosity measurement:** The slag was put into the crucible fixed by a pedestal in the furnace. The reducing atmosphere was provided by the mixture of  $\text{CO}_2$  and  $\text{CO}$ . To control the steady furnace temperature,

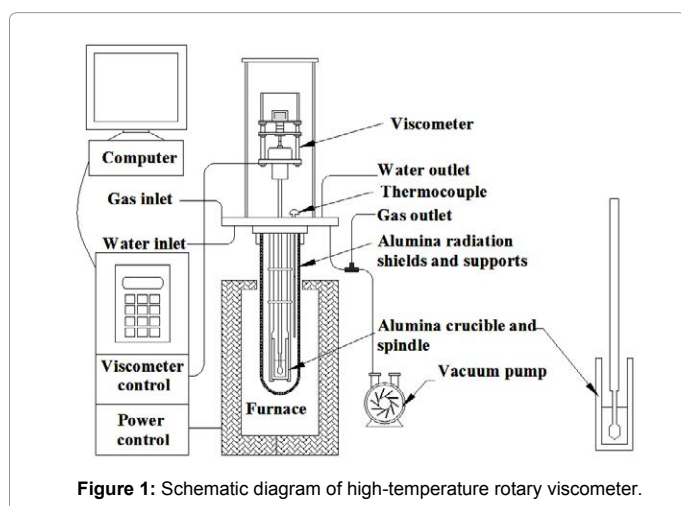


Figure 1: Schematic diagram of high-temperature rotary viscometer.

the heating rate was 10°C/min below 1200°C and 4°C/min above 1200°C. The viscosity measurements were started at the fully molten temperature until the slag viscosity exceeded 150 Pa·s. Besides, the rotational speed and viscosity were recorded automatically.

**Rheology measurement:** The rheological characteristics of the slag, represented by the relationship between shear stress and shear rate were determined by the high-temperature rheometer. The specific procedure was as following. The slag was firstly loaded into crucible, and then heated to the test temperature at which heating continued for at least 1 hr to ensure that the whole slag sample achieved a state of thermal equilibrium. The spindle was put into the molten liquid slag. Test was conducted by rotating the spindle at a low speed and the torque acting on the spindle was measured. The rotational speed was increased in steps from the minimum value to the maximum value and then decreased in steps from the maximum value to the minimum value. During the process, the rotational speed and the torque response at each constant speed was recorded.

### FactSage simulation

In this study, the liquidus temperature, proportions of solids, and mineral formation for the multi-component system ( $\text{SiO}_2$ - $\text{Al}_2\text{O}_3$ - $\text{CaO}$ - $\text{Fe}_2\text{O}_3$ - $\text{MgO}$ - $\text{TiO}_2$ - $\text{Na}_2\text{O}$ - $\text{K}_2\text{O}$ ) were calculated by the thermodynamic software FactSage [22]. The calculation results between 1000°C and 1600°C under reducing atmosphere at 1 atm pressure are obtained. The calculation principle of FactSage is based on Gibbs' energy minimization at a given temperature and compositional range.

## Results and Discussion

### Slag sample characteristic

**Chemical composition of the slag:** The composition of slag determined by XRF is shown in Table 1. The content of basic oxides ( $\text{CaO}+\text{Fe}_2\text{O}_3+\text{MgO}+\text{Na}_2\text{O}+\text{K}_2\text{O}$ ) is above 68%, which is attributed to the higher liquid's temperature.

**Mineral constituent of the slag:** The X-ray diffractograms of the slag and the coal ash are shown in Figure 2. It can be seen that the mineral matters of slag are different from those of the coal ash. The mineral matters of the coal ash are mainly anhydrite, quartz, hematite, calcite and lime. The mineral matter peaks of coal ash are obvious and the diffraction intensity is strong with the range of 2000-7000 CPS. However, the mineral matter peaks of slag are not obvious and the diffraction intensity is weak with the range of 50-100 CPS. It shows that the slag has minor mineral matter and behaves mainly an amorphous character. Thus, the slag is fully molten during the preparation. This behavior is similar to the behavior of the actual slag in industry.

**Microstructure of the slag:** The SEM pictures of coal ash and the slag are shown in Figure 3. It can be seen that the surface of the slag is distinct from that of the coal ash. The surface of the coal ash is coarse and there are lots of crystalline particles. However, the surface of the slag is more smooth and there is little crystalline particle. It reveals that the slag is molten during the preparation, which is consistent with the XRD results.

### Viscosity of the slag

The optimal viscosity for successful slagging of the entrained-flow gasifier is 15 Pa·s, and especially less than 25 Pa·s at the tapping temperature [8]. Figure 4 shows the slag viscosity variation with the change of temperature. It can be seen from Figure 4 that the viscosity is lower than 5 Pa·s when the temperature is higher than 1380°C and

Ash chemical composition Wt/%	SiO <sub>2</sub>	Al <sub>2</sub> O <sub>3</sub>	Fe <sub>2</sub> O <sub>3</sub>	CaO	MgO	Na <sub>2</sub> O	K <sub>2</sub> O	SO <sub>3</sub>	TiO <sub>2</sub>	Others
	27.80	13.49	15.19	27.10	2.49	1.36	0.42	10.04	0.50	1.61

Table 1: Ash chemical composition of Yulin slag.

the viscosity increases dramatically at the temperature of critical viscosity ( $T_{cv}$ ) 1340°C. In other words, tapping temperature must be above 1340°C to ensure that the slag flows smoothly under the force of gravity. Thus, the temperature range of rheology experiment is chosen from 1360°C to 1460°C.

### Rheology of the slag

**Effect of shear rate on shear stress:** The shear stress of slag as a function of shear rate at different temperatures is shown in Figure 5. From Figure 6, it is apparent that the linear relationship between shear stress and shear rate is found in the range of 1380-1460°C and the nonlinear relationship between shear stress and shear rate is observed in the range of 1360-1370°C. It indicates that the fluid shows the Newtonian behavior at the temperature of 1380-1460°C, while the fluid displays non-Newtonian behavior at the temperature of 1360-1370°C. These results agree well with the discussions represented by Figure 5.

**Effect of shear rate on viscosity:** The rheology experiments of the slag were carried out in a reducing atmosphere with the temperature range of 1360°C-1460°C. Figure 5 shows the viscosity as a function of shear rate and temperature. As illustrated in Figure 5(a), the viscosity of slag is basically constant at the shear rate of 5-50s<sup>-1</sup> and a small deviation from the constant occurs at the shear rate of 0-5s<sup>-1</sup> when the temperature is in the range of 1380°C-1460°C. As a result of the crystalline particles disorder direction at low shear rate, the viscosity tends to keep constant at higher shear rate. Therefore, the viscosity of slag can be regarded as basically constant at the whole shear rate range, which shows that the slag behaves as Newtonian fluid. It can also be seen from Figure 5(b) that the viscosity decreases dramatically with increasing shear rate when the temperature decreases to 1370°C and 1360°C. For example, the viscosity of slag is about 30 Pa·s at the 2s<sup>-1</sup> shear rate and it is about 10 Pa·s at the 20s<sup>-1</sup> shear rate when the temperature is 1360°C. This behavior is called "shear thinning" and it usually occurs in particulate suspensions and polymer melts [23]. The behavior attributes to the occurrence of crystalline particles in the slag with the decreasing temperature. The increase of shear rate leads to the crystalline particles parallel to the flow direction and thus resulting in the viscosity decreases [24].

In addition, the viscosity decreases with increasing temperature at any constant shear rate. It is apparent that the viscosity of slag is 15 Pa·s at the 10s<sup>-1</sup> shear rate when the temperature is 1360°C. The viscosity of slag decreases to 0.3 Pa·s at the 10s<sup>-1</sup> shear rate when the temperature is 1460°C.

**Fluid models and mineral variation at different temperatures:** The flow types are evaluated for the study on the rheological properties of fluid. The main classifications of fluids are the time-independent fluids and time-dependent fluids. The time-independent fluid that is undergone a stress for a period of time behaves the same viscosity while the time-dependent fluid shows the different viscosity. Most slag is time-dependent fluid and this behavior directly relates to the rheology. The classical fluid models presenting the relationship between shear stress and shear rate are as follows [10]:

$$\text{Newtonian model: } \sigma = \mu\dot{\gamma} \quad (1)$$

$$\text{Casson model: } \sigma = \sigma_0 + \eta_0\dot{\gamma}^n \quad (2)$$

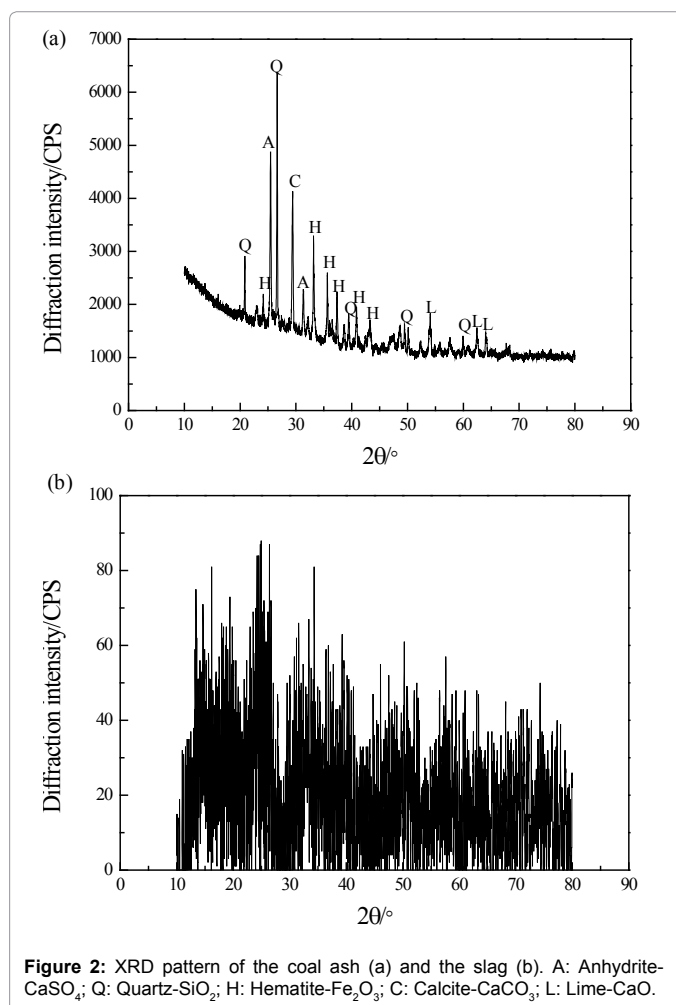


Figure 2: XRD pattern of the coal ash (a) and the slag (b). A: Anhydrite-CaSO<sub>4</sub>; Q: Quartz-SiO<sub>2</sub>; H: Hematite-Fe<sub>2</sub>O<sub>3</sub>; C: Calcite-CaCO<sub>3</sub>; L: Lime-CaO.

$$\text{Hershel-Bulkley model: } \sigma = \sigma_0 + \eta_0\dot{\gamma}^n \quad (3)$$

As shown in Table 2, the relationships of the shear stress and shear rate at different temperatures are fitted. The correlation coefficients in Table 2 are above 0.95, which indicates that the fitted values agree well with the experimental values.

As shown in Figure 7, the relative minerals content and the solid/liquid-phase relative content as a function of temperature is calculated by FactSage, where the dash line is the volume fraction of crystalline particles expressed by  $\phi$ . It can be seen from Figure 7 that the proportion of liquid-phase in the slag decreases and the minerals increase as the temperature decreases. When the temperature is lower than 1380°C, the proportion of solid-phase and the volume fraction of crystalline particles increase rapidly as the temperature decreases. The volume fraction of crystalline particles increases from 18% to 40% when the temperature decreases from 1360°C to 1300°C. However, the volume fraction of crystalline particles is lower than 10% and the proportion of solid-phase increases slowly as temperature decreases when the temperature is higher than 1380°C. It can be seen that the volume fraction of crystalline particles increases from 5% to 9.7% when the temperature decreases from 1460°C to 1380°C. It is the reason why

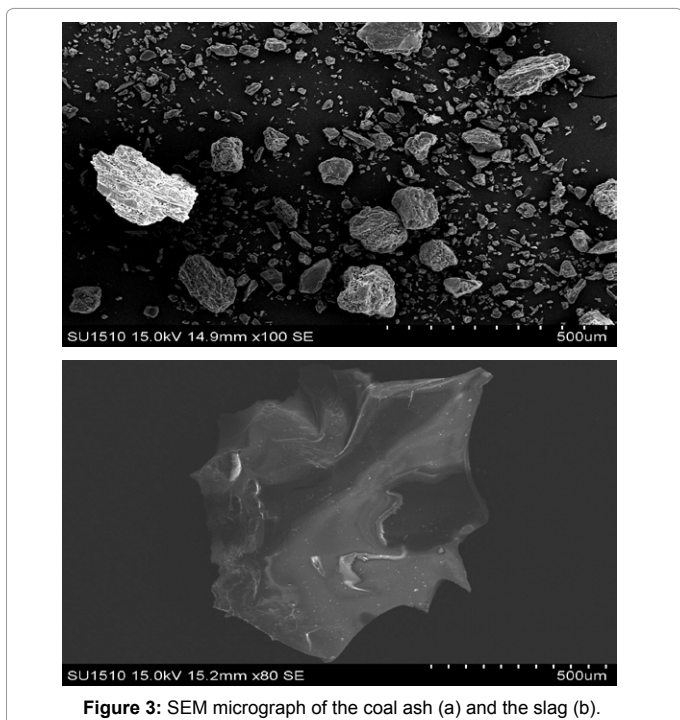


Figure 3: SEM micrograph of the coal ash (a) and the slag (b).

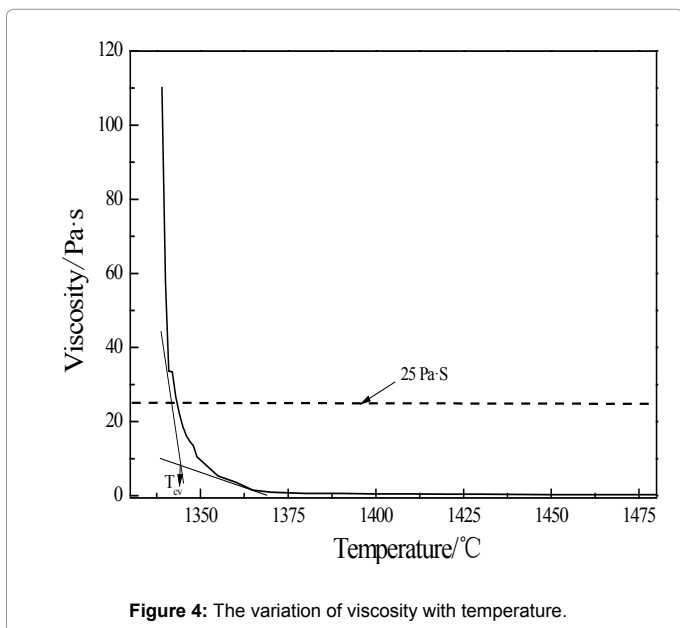


Figure 4: The variation of viscosity with temperature.

Temperature/°C	Model	Equation	R <sup>2</sup>
1460	Newtonian	$\sigma=0.310\gamma$	0.996
1440	Newtonian	$\sigma=0.417\gamma$	0.987
1420	Newtonian	$\sigma=0.585\gamma$	0.988
1400	Newtonian	$\sigma=0.747\gamma$	0.986
1380	Newtonian	$\sigma=1.004\gamma$	0.989
1370	Casson	$\sigma^{1/2}=5.711^{1/2}\gamma^{1/2}+6.763^{1/2}$	0.986
1360	Hersehel-Bulkley	$\sigma=39.499\gamma^{0.523}-2.300$	0.960

Table 2: Models for the description of fluid behavior at different temperatures.

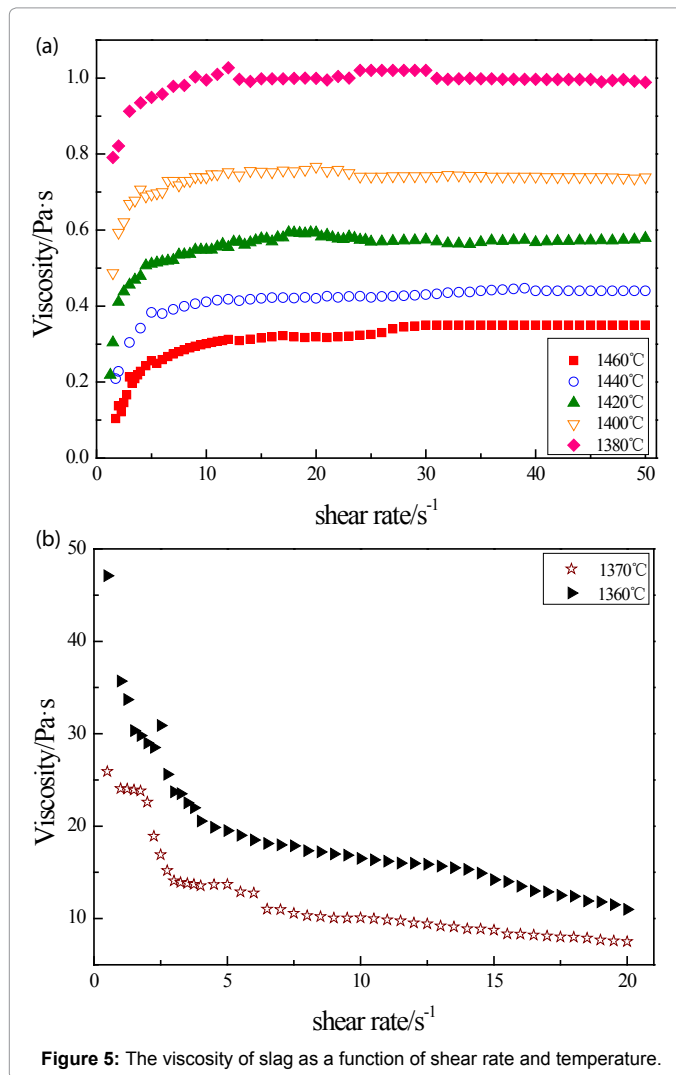


Figure 5: The viscosity of slag as a function of shear rate and temperature.

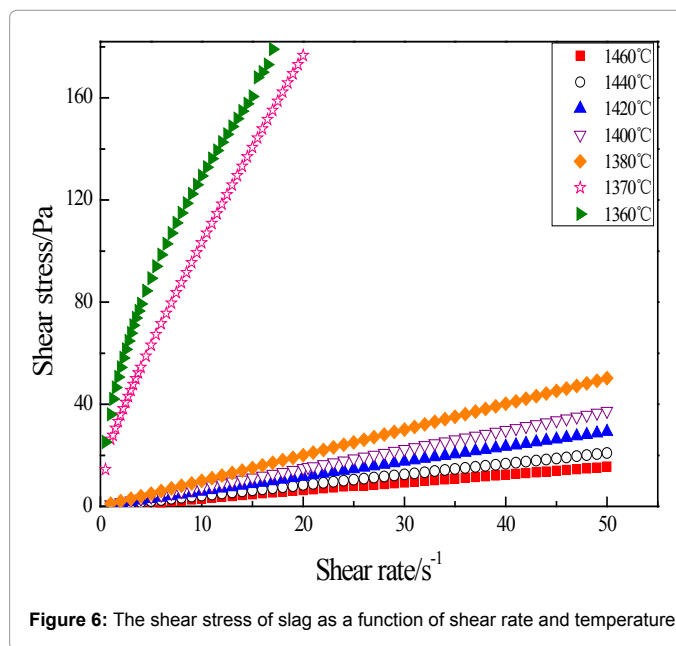


Figure 6: The shear stress of slag as a function of shear rate and temperature.

the slag viscosity increases rapidly as temperature decreases at lower temperatures, but increases slowly as temperature decreases at higher temperatures.

**Thixotropy of slag:** The thixotropy property of the slag refers to the behavior that the viscosity continues to decrease for a period of time under constant shear rate, and displays recovery gradually after the shear stress is canceled [25]. For a slag with thixotropic behavior, there is a formed hysteresis loop when the shear rate is increased stepwise from zero to some maximum value and then goes back to zero steadily. Figure 8 presents the relationship between the shear stress and shear rate at temperature of 1360°C-1460°C where the I refer to the measurement in the shear rate increasing process and the D refers to the measurement in the shear rate decreasing process. Due to the measuring range of torque, the shear rate increases from zero to the 50s<sup>-1</sup>, and then decrease from 50s<sup>-1</sup> to zero when the temperature is above 1380°C. Because of mass crystalline particles formed, the maximum value that shear rate achieved is 20s<sup>-1</sup> when the temperature is 1360°C and 1370°C. It indicates from Figure 8 that when the temperature is in the range of 1380°C-1460°C the slag behaves as a Newtonian fluid and there is no a hysteresis loop. And it is also consistent with the results shown in Figure 6. Furthermore, Figure 7 shows that the volume fraction of crystalline particle at 1380°C is 9.7%. That is to say, when the volume fraction of crystalline particle is lower than 10%, the slag presents as Newtonian fluid. When the temperature decreases to 1360°C and 1370°C with the volume fraction of crystalline particle is 18% and 16%, hysteresis loops occur in the slag with crystalline particles. The area of hysteresis loops with 1360°C is larger than that of 1370°C, which shows that the more crystallize particles form in lower temperature. As the temperature decreases, the alignment of crystalline particles increases which breaks up the interaction of internal particles and increases the fraction of maximum packing [26]. Those contribute to the appearance of hysteresis loops. Under the shear stress, the microstructure of mixture is broken up and recovers at rest which may be the cause for the higher shear stress of a slag in increasing shear rate process than in decreasing shear rate process.

### Viscosity prediction

Based on S<sup>2</sup> model and Einstein-Roscoe model, the predicted model of bituminous coal slag has been established. The model can be expressed by  $\eta = 0.0144\eta_n(1 - 1.35\frac{\phi}{\phi_n})^{-17.9952} + 0.5659$ . The detailed calculation process is shown as follows.

**Completely molten models:** The completely molten models have been used to predict the viscosity of slag and compared with the experimental values shown in Figure 9. It can be seen from Figure 9 that when the temperature is higher than 1380°C the predicted values of S<sup>2</sup>, Streeter, Watt-Fereday and Shaw models agree well with the experimental values. But a large number of crystalline particles appear in the slag which results in the models inapplicability when the temperature is lower than 1370°C.

The predicting effect of the S<sup>2</sup>, Streeter, Watt-Fereday and Shaw models can be evaluated by the bias and standard errors, and the standard error  $\sigma_s$  and determination coefficient R<sup>2</sup> are calculated from the following:

$$\sigma_s = \sqrt{\frac{n}{n-1} \sum_{i=1}^n (y_i - p_n(x_i))^2} \quad (4)$$

$$R^2 = 1 - \frac{\sum_{i=1}^n (y_i - p_n(x_i))^2}{\sum_{i=1}^n (y_i - \bar{y})^2} \quad (5)$$

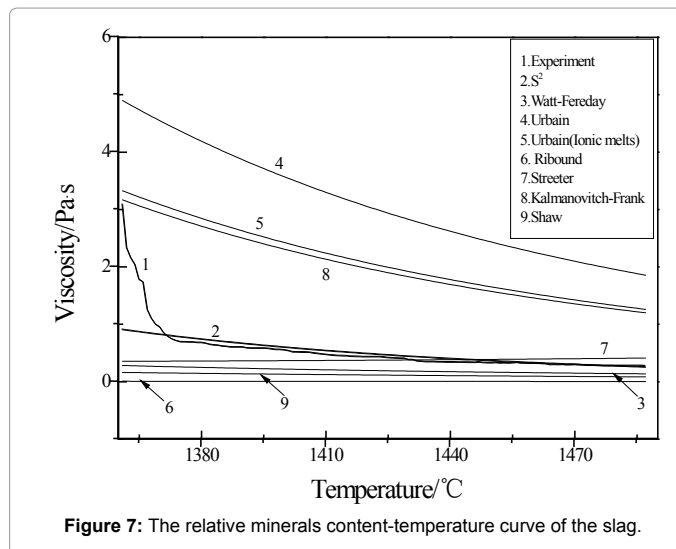


Figure 7: The relative minerals content-temperature curve of the slag.

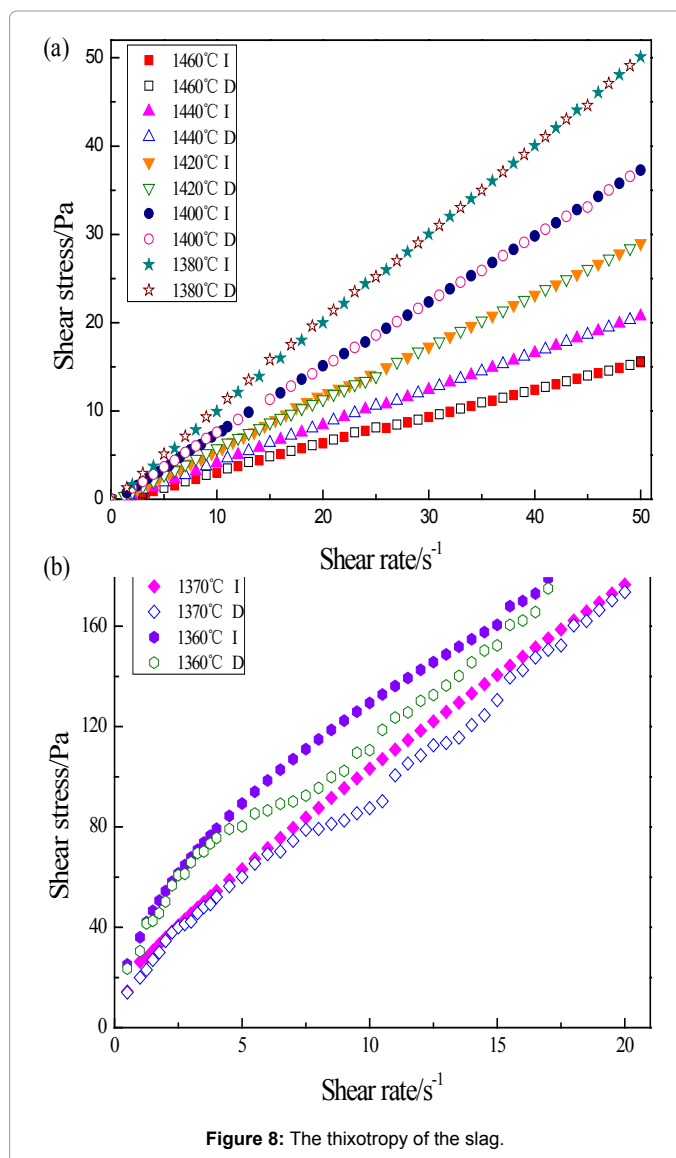


Figure 8: The thixotropy of the slag.

In general, when  $R^2$  and  $\sigma_s$  approach 1 and zero, respectively, the predicted values are close to the experimental values.

The values of  $R^2$  and  $\sigma$  for the  $S^2$ , Streeter, Watt-Fereday and Shaw models are illustrated in Table 3. From Table 3, it can be seen that the standard error  $\sigma_s$  and determination coefficient  $R^2$  of the  $S^2$  model are 0.79 and 0.37, respectively. The predicting effect of the  $S^2$  model is the best compared to other models. However, the viscosity of slag containing a lot of crystalline particles can't be predicted by the  $S^2$  model. Therefore, there is need to modify the  $S^2$  model for the accurate prediction of the slag viscosity.

**Liquid-solid mixtures models:** Due to the inaccurate prediction of the  $S^2$  model indicated in Figure 9, it is necessary to establish the viscosity model based on solid-liquid mixtures models. The models widely used for predicting the viscosity of liquid-solid mixtures are as follows [7]:

$$\text{Einstein: } (\eta_s - \eta) / \eta = 2.5\phi \quad (6)$$

$$\text{Einstein-Roscoe: } \eta_s = \eta(1 - c \cdot \frac{\phi}{\phi_m})^{-5/2} \quad (7)$$

$$\text{Chong: } \frac{\eta_s}{\eta} = \left[ 1 + 0.75 \cdot \frac{\phi}{\phi_m - \phi} \right]^2 \quad (8)$$

$$\text{Vand: } \eta_s = \eta \cdot (1 + 2.5 \cdot \theta + 7.349 \cdot \theta^2) \quad (9)$$

In this study,  $\phi_m$  is equal to 1 and the value of  $c$  is 1.35. The relative content of the composition in the liquid as a function of temperature, calculated by FactSage, is shown in Figure 10. The composition of the liquid can be used to calculate the viscosity of completely molten silicates and then the viscosity of liquid-solid mixtures can be obtained.

Based on the thermodynamic calculated values in Figure 10 and  $S^2$  model, the predicted viscosity of solid-liquid mixtures are shown in Figure 11 where E- $S^2$  means that the solid-liquid mixtures model is Einstein and the molten viscosity model is  $S^2$  and the same way for E-R- $S^2$ , C- $S^2$ , V- $S^2$ .

From Figure 11, it indicates that the solid-liquid mixture models predictions are in agreement with the experimental values when the volume fraction is lower than 15% and the temperature is higher than 1370°C. It also implies that the solid-liquid mixtures model can predict accurately the experimental values only when the volume fraction of crystalline particles is lower than 15%, which is consistent with the literature [7]. Further, the E-R- $S^2$  is the most close to the experimental values. Therefore, the experimental values are modified according to E-R- $S^2$  and the comparison between the experimental values and prediction values is shown in Figure 12. The predicted model is as following:

$$\eta = 0.0144\eta_s(1 - 1.35 \frac{\phi}{\phi_m})^{-17.9952} + 0.5659 \text{ where } R^2=0.9947 \quad (10)$$

Therefore, the formula is suitable for the slag viscosity prediction in the whole temperature range.

## Conclusions

In this study, rheological measurements of the slag in reducing atmosphere were conducted at the temperature range of 1360°C-1460°C and the viscosity prediction model of the slag was established on the basis of the  $S^2$  model and solid-liquid mixtures Einstein-Roscoe. The software FactSage was used to calculate the solid-liquid relative contents and the volume of crystalline particles at different

temperature. As temperature decreases, the viscosity and shear stress of the slag increase at the constant rotation speed. When the volume fraction of the crystallize particles is less than 10%, the slag behaves as a Newtonian fluid. When the volume fraction of the crystalline particles is more than 15%, the viscosity of slag decreases with increasing shear rate. In addition, the shear thinning behavior and thixotropic behavior are investigated which represent the non-Newtonian fluid characteristics of slag. Moreover, the viscosity model basing on the  $S^2$  model and Einstein-Roscoe model was established to accurate predict the viscosity of the bituminous slag in the whole temperature range.

## Acknowledgments

This work is partially supported by National Nature Science Foundation of China (Grant 21176078).

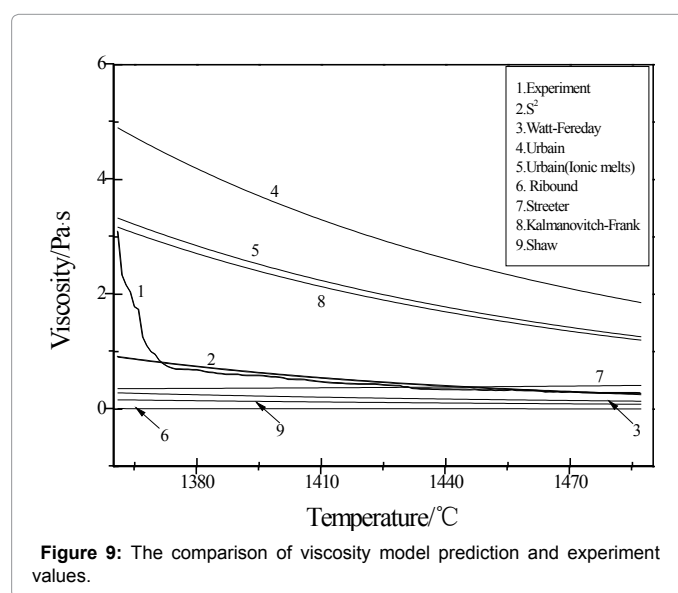


Figure 9: The comparison of viscosity model prediction and experiment values.

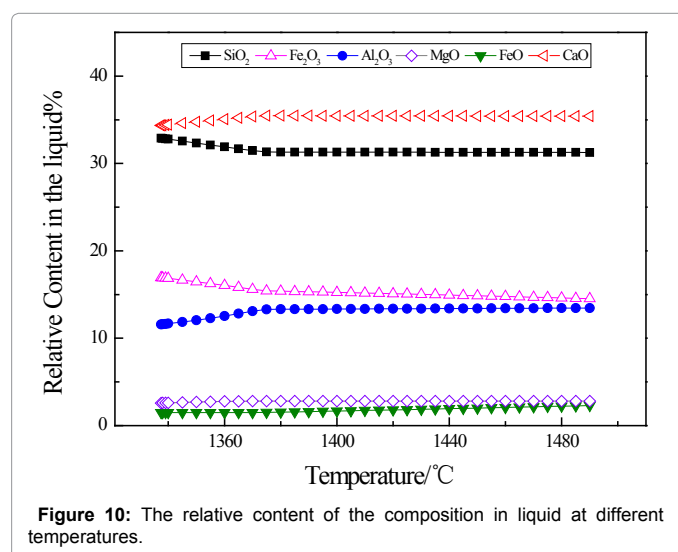


Figure 10: The relative content of the composition in liquid at different temperatures.

Sample	$S^2$		Watt-Fereday		Streeter		Shaw	
	$R^2$	$\sigma$	$R^2$	$\sigma$	$R^2$	$\sigma$	$R^2$	$\sigma$
Slag	0.79	0.37	0.70	2.01	0.68	2.58	0.37	4.73

Table 3: The value of  $R^2$  and  $\sigma$  for empirical models.

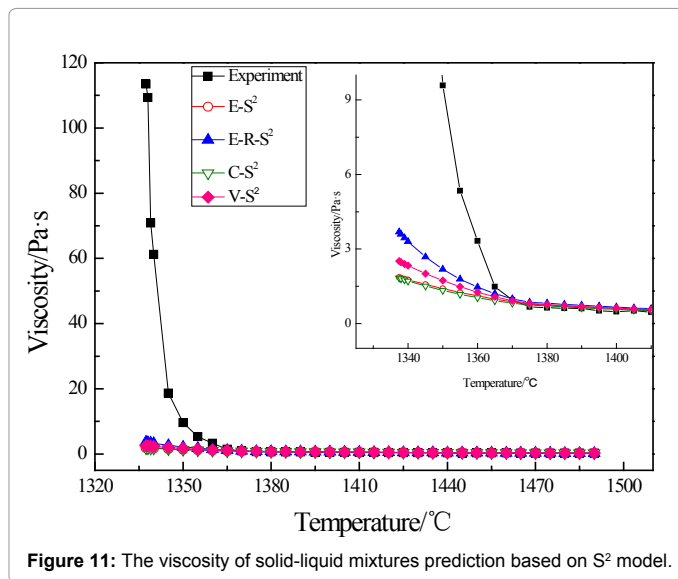


Figure 11: The viscosity of solid-liquid mixtures prediction based on  $S^2$  model.

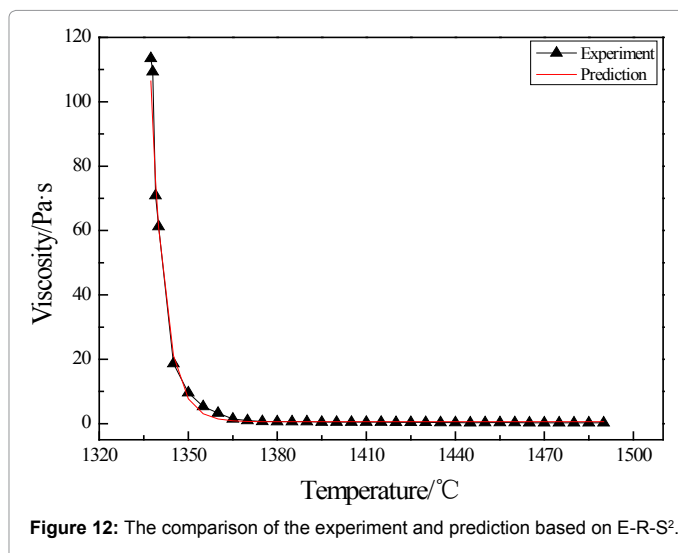


Figure 12: The comparison of the experiment and prediction based on E-R-S<sup>2</sup>.

## Nomenclature

$\mu$	viscosity coefficient
$\eta$	viscosity of completely molten silicates(Pa·s)
$\eta_0$	plastic viscosity (Pa·s)
$\eta_s$	real viscosity(Pa·s)
$\gamma$	shear rate ( $s^{-1}$ )
$\sigma$	shear stress(Pa)
$\sigma_0$	yield stress(Pa)
$\sigma_s$	the standard error
$\varphi, \theta$	volume fraction of the crystallize particles
$y_i$	experimental value,
$P_n(x_i)$	predicted values of models
$\overline{P_n(x_i)}$	average of the calculated values
IGCC	integrated gasification combined cycle
$R^2$	determination coefficient

SEM	scanning electron microscopy
$T_{cv}$	the temperature of critical viscosity
XRF	X-ray fluorescence
XRD	X-ray diffraction

## References

- Papic MM (1976) Technology and economics of coal gasification. Canadian Journal of Chemical Engineering 54: 413-420.
- Chen CX, Miyoshi T, Kamiya H, Horio M, Kojima T (1999) On the scaling-up of a two-stage air blown entrained flow coal gasifier. Canadian Journal of Chemical Engineering 77: 745-750.
- Beer JM (2007) High efficiency electric power generation the environmental role. Progress in Energy and Combustion Science 33: 107-134.
- Minchener J (2005) Coal gasification for advanced power generation. Fuel 84: 2222-2235.
- Gupta RP (2005) Coal research in Newcastle-past present and future. Fuel 84: 1176-1188.
- Farley JM (2007) Clean coal technologies for power generation. Energy Materials 2: 134-138.
- Bryant GW, Lucas JA, Gupta SK, Wall TF (1998) Use of thermomechanical analysis to quantify the flux additions necessary for slag flow in slagging gasifiers fired with coal. Energy Fuels 12: 257-261.
- Browning GJ, Bryant GW, Hurst HJ, Lucas JA, Wall TF (2003) An empirical method for the prediction of coal ash slag viscosity. Energy Fuels 17: 731-737.
- Kim MR, Jang JG, Lee SK, Hwang BY, Lee JK (2010) Correlation between the ash composition and melting temperature of waste incineration residue. Korean Journal of Chemical Engineering 27: 1028-1034.
- Vargas S, Frandsen FJ, Johansen K Dam (2001) Rheological properties of high-temperature melt of coal ashes and other silicates. Progress in Energy and Combustion Science 27: 237-429.
- Atesok G, Ozer M, Burat F, Dincer Atesok H (2012) Investigation on interaction of combustion parameters of coal-water mixtures used in fluidized bed combustor. International Journal of Coal Preparation and Utilization 32: 57-68.
- Hurst HJ, Novak F, Patterson JH (1999) Viscosity measurements and empirical predictions for fluxed Australian bituminous coal ashes. Fuel 78: 1831-1840.
- Van Dyk JC, Waanders FB, Benson SA, Laumb ML, Hack K (2009) Viscosity predictions of the slag composition of gasified coal utilizing FactSage equilibrium modeling. Fuel 88: 67-74.
- Yuan HP, Liang QF, Gong X (2012) Crystallization of Coal ash slags at high temperatures and effects on the viscosity. Energy Fuels 26: 3717-3722.
- Buhre BJP, Browning GJ, Gupta RP, Wall TF (2005) Measurement of the viscosity of coal-derived slag using thermomechanical analysis. Energy Fuel 19: 1078-1083.
- Nowok JW, Hurley JP, Stanley DC (1993) Local structure of a lignitic coal ash slag and its effect on viscosity. Energy Fuels 7: 1135-1140.
- Nowok JW (1995) Viscosity and structural state of iron in coal ash slags under gasification conditions. Energy Fuels 9: 534-539.
- Folkedahl BC, Schobert HH (2005) Effects of atmosphere on viscosity of selected bituminous and low-rank coal ash slags. Energy Fuels 19: 208-215.
- Schobert HH, Streeter RC, Diehl EK (1985) Flow properties of low-rank coal ash slags implications for slagging gasification. Fuel 64: 1611-1617.
- Tonmukayakul N, Nguyen QD (2002) A new rheometer for direct of measurement of the flow properties of coal ash at high temperatures. Fuel 81: 397-404.
- Song WJ, Tang LH, Zhu XD, Wu YQ, Zhu ZB, Koyama S (2010) Flow properties and rheology of slag from coal gasification. Fuel 89: 1709-1715.
- Bale CW, Chartrand P, Degterov SA, Eriksson G, Hack K, et al. (2002) FactSage thermochemical software and databases. Calphad 26: 189-228.
- Sunand N, Kee DDe (2001) Simple shear, hysteresis and yield stress in biofluids, Canadian Journal of Chemical Engineering 79: 36-41.

24. Wright S, Zhang L, Sun S, Jahanshahi J (2000) Viscosity of a CaO-MgO-Al<sub>2</sub>O<sub>3</sub>-SiO<sub>2</sub> melt containing spinel particles at 1646 K. *Metallurgical and Materials Transactions B* 31: 97-104.
25. Bourmonville B, Nzihou A (2002) Rheology of non-Newtonian suspensions of fly ash: effect of concentration, yield stress and hydrodynamic interactions. *Powder Technology* 128: 148-158.
26. Yue YM, Russel C (1999) Influence of suspended iso-and anisometric crystals on the flow behavior of fluoroapatite glass melts during extrusion. *Physics and Chemistry of Glasses* 40: 243-247.